J|A|C|S
ARTICLES
Published on Web 09/03/2003

The Structure of NADH in the Enzyme dTDP-D-glucose Dehydratase (RmlB)

Konstantinos Beis,[1] Simon T. M. Allard,[1,2] Adrian D. Hegeman,[2] Garib Murshudov,[3] Douglas Philp,*[,1] and James H. Naismith*[,1]

Contribution from the Centre for Biomolecular Sciences, University of St. Andrews, North Haugh, St. Andrews, Fife KY16 9ST, United Kingdom, the Department of Biochemistry, University of Wisconsin-Madison, Madison, Wisconsin 53706, and the Structural Biology Laboratory, Department of Chemistry, University of York, York YO10 5DD, United Kingdom

Received April 25, 2003; E-mail: d.philp@st-andrews.ac.uk; naismith@st-and.ac.uk.

Abstract: The structure of *Streptococcus suis* serotype type 2 dTDP-D-glucose 4,6-dehydratase (RmlB) has been determined to 1.5 Å resolution with its nicotinamide coenzyme and substrate analogue dTDP-xylose bound in an abortive complex. During enzyme turnover, NAD^+ abstracts a hydride from the C4′ atom of dTDP-glucose-forming NADH. After elimination of water, hydride is then transferred back to the C6′ atom of dTDP-4-keto-5,6-glucosene-regenerating NAD^+. Single-crystal spectroscopic studies unambiguously show that the coenzyme has been trapped as NADH in the crystal. Electron density clearly demonstrates that in contrast to native structures of RmlB where a flat nicotinamide ring is observed, the dihydropyridine ring of the reduced cofactor in this complex is found as a boat. The *si* face, from which the *pro-S* hydride is transferred, has a concave surface. Ab initio electronic structure calculations demonstrate that the presence of an internal hydrogen bond, between the amide NH on the nicotinamide ring and one of the oxygen atoms on a phosphate group, stabilizes this distorted conformation. Additionally, calculations show that the hydride donor ability of NADH is influenced by the degree of bending in the ring and may be influenced by an active-site tyrosine residue (Tyr 161). These results demonstrate the ability of dehydratase enzymes to fine-tune the redox potential of NADH through conformational changes in the nicotinamide ring.

Introduction

Nicotinamide adenine dinucleotide (NAD(H)) redox reactions are ubiquitous in biology. NAD^+ is most commonly found as a cofactor where it reversibly oxidizes various substrates by the removal of hydride from substrate. In addition to being found as a cofactor, NAD(H) can also be found as a coenzyme where it is not dissociated from the enzyme or consumed during turnover and where its redox state cycles during turnover. It has long been established that the basis of the redox properties is the destruction or formation of aromaticity of nicotinamide by the gain or loss of hydride from the C4 position of the pyridine ring. Aromatic rings are by definition planar, and very high-resolution neutron and X-ray studies confirm that the pyridine ring in NAD^+ is planar. Nonaromatic rings can, however, exhibit a variety of conformations.

Chemical studies have shown that the hydride carrier is the C4 atom on the pyridine ring of the nicotinamide and that the transfer[4] is stereospecific, depending on the protein; some proteins transfer the *pro-S* hydrogen atom as hydride, others the *pro-R*. A variety of theoretical methods have been applied[5] to NADH hydride transfer systems. These calculations have shown that ring puckering can greatly enhance the rate of hydride transfer by altering[6] the redox potential for the NAD^+/NADH couple. It is well-known that the extent of the puckering of the dihydropyridine ring is dependent upon its local environment. Although there are many NADH-containing protein structures known, a major difficulty is that at medium resolution (2.0 Å), geometric restraints dominate the observed geometry of nicotinamide rings. The first experimental evidence on the distortion of the NADH pyridine ring to optimize hydride transfer was reported[7] by Meijers et al. They reported the very high-resolution (1.1 Å) structure of horse liver alcohol dehydrogenase (LADH; EC.1.1.1.1) in complex with NAD(H). LADH is a class A dehydrogenase which catalyzes *pro-R* hydride removal from alcohol and *re* face addition of hydride to NAD^+. Their study showed that a hydroxide anion contacts the C2 of the nicotinamide ring, and subsequent theoretical calculations show that it is this hydroxide ion that puckers and twists the ring. The C4 atom is removed from the plane of the ring, but the nitrogen atom remains largely in the ring.

Most NAD(P)H-containing enzymes have no hydroxide ion to tune the redox potential. The most notable class of such

(1) University of St. Andrews.
(2) University of Wisconsin-Madison.
(3) University of York.
(4) (a) Fisher, H. F.; Conn, E. E.; Vennesland, B.; Westheimer, F. H. *J. Biol. Chem.* **1953**, *202*, 687−697. (b) Nambiar, K. P.; Stauffer, D. M.; Kolodziej, P. A.; Benner, S. A. *J. Am. Chem. Soc.* **1983**, *105*, 5886−5890.
(5) Wu, Y.-D.; Houk, K. N. *J. Am. Chem. Soc.* **1991**, *113*, 2353−2358.
(6) Almarsson, Ö.; Bruice, T. C. *J. Am. Chem. Soc.* **1993**, *115*, 2125−2138.
(7) Meijers, R.; Morris, R. J.; Adolph, H. W.; Merli, A.; Lamzin, V. S.; Cedergreen-Zeppezauer, E. S. *J. Biol. Chem.* **2001**, *276*, 9316−9321.

10.1021/ja035796r CCC: $25.00

enzymes is the short-chain dehydrogenase superfamily (SDR) of enzymes, which are ubiquitous in biology.[8] These enzymes bind NAD(P)H and are defined by the presence of a catalytic triad of Lys, Tyr, and Thr(Ser). The mechanism and structures of this class of enzymes have been intensively studied, yet there is no detailed experimental information on the structure of NAD(P)H in these systems.[9] Therefore, there are no data upon which theoretical calculations on the redox properties of NAD(P)H in enzymes can be based.

We aim to understand the chemistry behind the transformation of glucose-1-phosphate into dTDP-rhamnose by the four enzymes of the rhamnose pathway.[10] Rhamnose is found in many pathogens, including the capsule of *Streptococcus suis* serotype type 2. This organism mainly infects swine but is also known to be zoonotic, causing human meningitis;[11] significantly, it is the rhamnose-containing capsule that is essential for virulence.[12] The second enzyme of the pathway is RmlB (dTDP-D-glucose 4,6-dehydratase EC: 4.2.1.46) whose product, dTDP-4-keto-6-deoxyglucose, is the starting point for all 6-deoxy sugar biosynthesis. The enzyme belongs to the SDR superfamily and, in contrast to LADH, utilizes the *si* face of NADH. A detailed structural investigation of the enzyme mechanism has been published.[13] During enzyme turnover, a hydride is extracted from the substrate by NAD^+ to form NADH. This hydride is then transferred back to sugar nucleotide to form the product and regenerate NAD^+. In RmlB, NAD^+ functions as a coenzyme rather than cofactor. By using the substrate analogue dTDP-xylose (Figure 1), we have trapped an abortive complex with NADH and obtained high-resolution X-ray diffraction data. In the complex, the dihydropyridine ring of the NADH coenzyme is found to be profoundly puckered. We describe this distortion, use theoretical calculations to show how this distortion is achieved, and predict how it alters the redox potential of the coenzyme by providing a model for hydride transfer in this enzyme superfamily.

Results and Discussion

The details of the native protein structure have already been reported,[14] and the orientations of key active-site residues in the protein are essentially unchanged from the description of the dTDP-glucose complex.[13] The dTDP-xylose complex is best thought of as the first step in the reaction, the abstraction of hydride from the C4′ position of dTDP-xylose to form NADH and dTDP-4-keto-xylose. dTDP-4-keto-xylose is incapable of further reaction, and thus one unit of dTDP-xylose reduces an equimolar amount of RmlB. Single-crystal visible spectroscopy has confirmed that NADH is present in the crystal. Electron density clearly shows dTDP-xylose rather than dTDP-4-keto-xylose in the active site, presumably because the dTDP-xylose is 100 times more concentrated than the dead-end product. As a result, it should be recognized that the complex we have is distorted from the true situation during turnover because dTDP-xylose has a hydroxyl and proton at C4′ rather than a carbonyl group. The C4 atom of NADH is 3.7 Å from the C4′ atom of dTDP-xylose.

We have already shown[13] that dTDP binding is sufficient and necessary to adjust the active geometry to position the key catalytic residues (Tyr 161, Lys 165, Thr 125). In particular, we pointed out[13] that Tyr 161 moves to act directly as the base. The position of NADH is unchanged from our earlier descriptions; its conformation is determined by a network interaction with the protein (Figure 1a).[13,14] As in all members of the SDR class enzyme, there is an internal hydrogen bond between the phosphate and the primary amide attached to the nicotinamide ring. This hydrogen bond is preserved despite the puckering of the ring. Table 1 reports the metrics that have been used to represent the distortion of nicotinamide rings. Four values are reported: ring rms (the overall rms deviation of the six ring atoms from a plane), α_C (the extent which the C4 atom is out of plane), α_N (extent which the N1 atom is out of plane), and twist (deviation from the boat form). In our structure, both the C4 and N1 atoms have moved significantly out of the plane of the ring. In the NAD^+-containing dTDP complex structure, the ring is flat,[14] indicating this boat distortion is not directly a result of the protein (whose structure remains essentially unchanged). The ring we observe is considerably more puckered than that seen for LADH; in particular, we see that the N1 atom has become significantly pyramidal and moved out of the plane. However, the NADH ring we observe in our structure is essentially untwisted. There are differences between the A and the B subunits, and it is notable that the ring is less distorted in the B subunit. We observed from the first maps that the electron density in this subunit was weaker and that the experimental

Table 1. Metrics Used To Determine Ring Pucker in Dihydropyridine Ring of NADH[a]

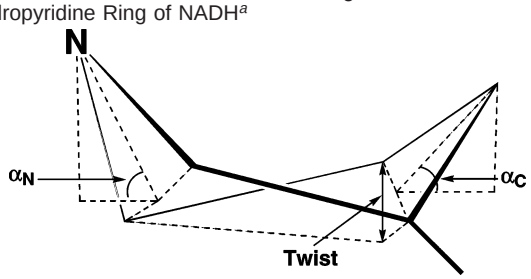

	rmsd/ Å[b]	α_C/ (deg)	α_N/ (deg)	twist/ Å	ESP at transferred H
subunit A	0.204	29	30	−0.06	−14.0[c]
subunit B	0.142	18	25	−0.03	−12.1[c]
calculated syn	0.143	21	26	−0.03	−8.2
calculated anti	0.022	5	7	0.00	+2.0
LADH[d]	0.14−0.17	9.2−13.8	3.0−8.9	0.37−0.57	−

[a] The diagram below defines the metrics used. Calculated structures are shown in Figure 2. [b] Rmsd is the rms deviation from the least-squares plane derived from the nonhydrogen atoms of the dihydropyridine ring.[c] These values are derived from single-point calculations in which the calculated syn structure was distorted manually to approximately the X-ray geometry. They serve to illustrate that the hydride becomes more available as the structure is distorted further, but the absolute values are probably not completely accurate. [d] Values observed in the high-resolution crystal structure of alcohol dehydrogenase.[7]

(8) Rossmann, M. G.; Liljas, A.; Bränden, C. I.; Banaszak, L. J. In *The Enzymes*; Boyer, P. D., Ed.; Academic Press: New York, 1975; pp 61−102.
(9) Labesse, G.; Vidal-Cros, A.; Chomilier, J.; Gaudry, M.; Mornon, J. P. *Biochem. J.* **1994**, *304*, 95−99.
(10) Giraud, M. F.; Naismith, J. H. *Curr. Opin. Struct. Biol.* **2000**, *10*, 687−696.
(11) Halaby, T.; Hoitsma, E.; Hupperts, R.; Spanjaard, L.; Luirink, M.; Jacobs, J. *Eur. J. Clin. Microbiol. Infect. Dis.* **2000**, *19*, 943−945
(12) Smith, H. E.; Damman, M.; van der Velde, J.; Wagenaar, F.; Wisselink, H. J.; Stockhofe-Zurwieden, N.; Smits, M. A. *Infect. Immun.* **1999**, *67*, 1750−1756.
(13) Allard, S. T. M.; Beis, K.; Giraud, M.-F.; Hegeman, A.; Gross, J. W.; Wilmouth, R. C.; Whitfield, C.; Graninger, M.; Messner, P.; Allen, A. G.; Maskell, D. J.; Naismith, J. H. *Structure* **2002**, *10*, 81−92.
(14) Allard, S. T. M.; Giraud, M.-F.; Whitfield, C.; Graninger, M.; Messner, P.; Naismith, J. H. *J. Mol. Biol.* **2001**, *307*, 283−295.

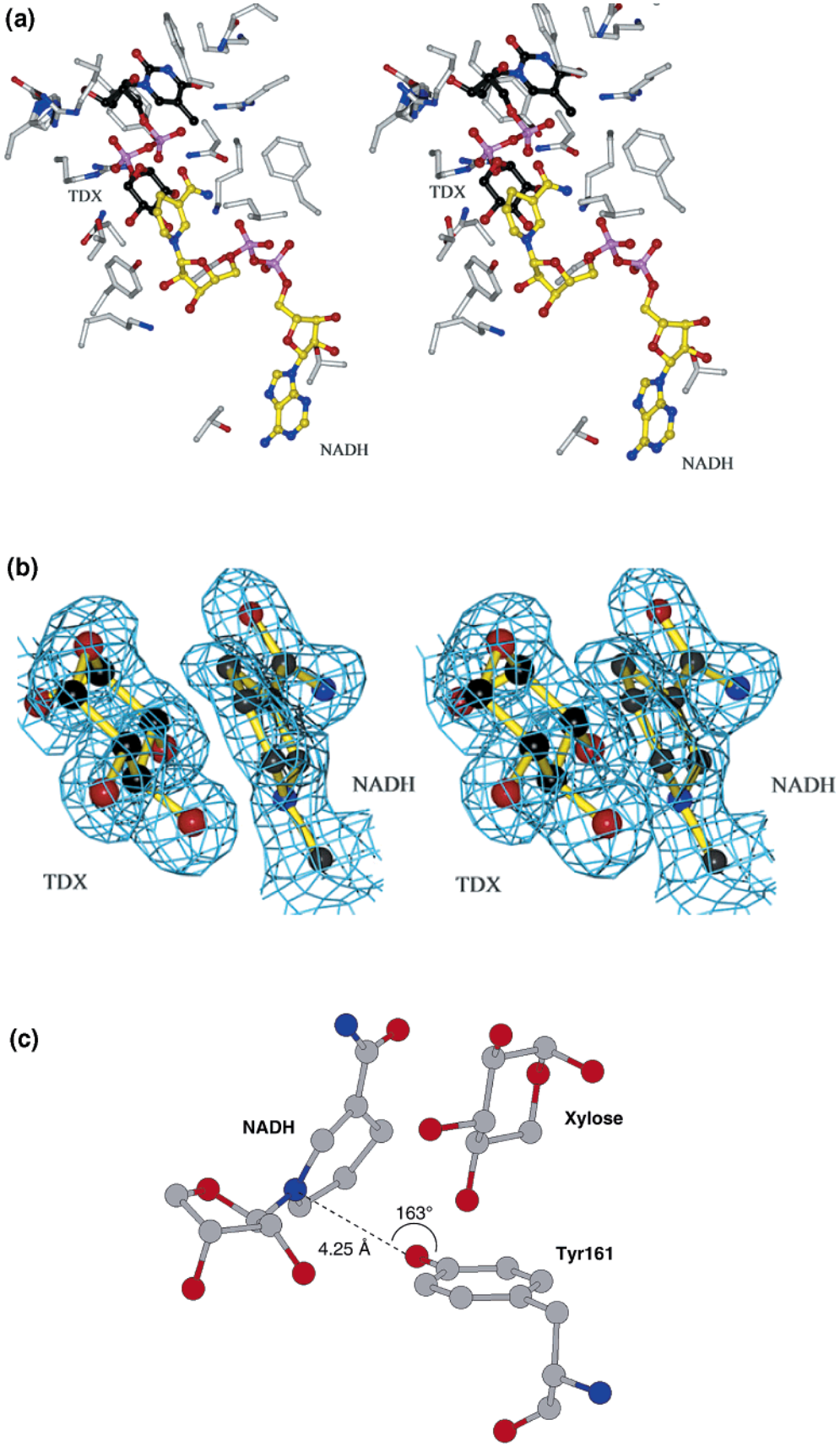

Figure 1. The structure of the complex between dTDP-xylose and RmlB. (a) Cross-eye stereo diagram of the NADH, dTDP-xylose (TDX), and RmlB protein complex in stick format. In NADH, carbon atoms are shown in yellow, oxygen red, phosphorus purple, and nitrogen blue. In dTDP-xylose carbon atoms are black and other atom colors are as in NADH. In the protein, carbon atoms are gray and other atoms are colored as in NADH. (b) Cross-eye stereo diagram of $F_o - F_c$ electron density for NADH and dTDP-xylose contoured at 3σ. The phases for the map were calculated on the model which had not previously included NADH or dTDP-xylose. (c) Local arrangement of the dihydropyridine ring of NADH with respect to Tyr161 in the abortive complex. Carbon atoms are shown as gray spheres, oxygen as red, nitrogen as blue, and phosphorus as purple. Distances and angles are derived from X-ray data.

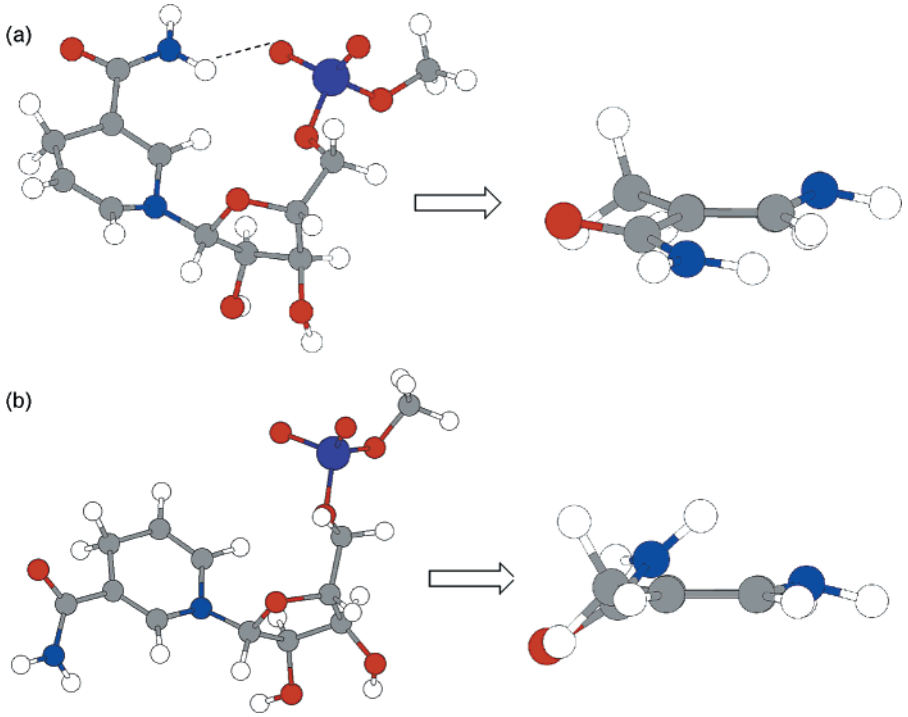

Figure 2. The calculated structures (MP2/6-31G(d,p)) of (a) the syn and (b) the anti forms of our model of the NADH structure. Carbon atoms are shown as gray spheres, oxygen as red, nitrogen as blue, hydrogen as white, and phosphorus as purple. Hydrogen bonds are shown in dotted lines. In each case the dihydropyridine ring is extracted and shown edge-on to allow the reader to gauge ring pucker accurately.

data are probably insufficiently strong to define the ring structure during restrained refinement. In both subunits, the C4 and C5 atoms have higher thermal parameters than the other atoms in the ring; this is consistent with large differences in the α_C values between the monomers (Table 1). Taken together, the data suggest that either this region of the ring is structurally flexible or some oxidized NAD^+ is also present.

In crypto-redox enzymes such as RmlB, there is no net transfer of hydride during the reaction. Rather, the hydride is abstracted from substrate, and the *pro-S* hydride is returned to some intermediate to form the final product. The tightly bound nicotinamide cycles between oxidized and reduced during turnover and is found oxidized in the resting state. Such a system provides a particularly useful tool in studying the behavior of the nicotinamide ring during turnover since both hydride abstraction and hydride transfer occur during a single enzyme turnover. The structure of NAD^+ is known from atomic resolution studies on proteins to be planar, most recently shown by a neutron diffraction study.[15] The accurate structure of NADH in a protein that both oxidizes and reduces during turnover provides a strong experimental basis for modeling the redox chemistry of a NAD^+/NADH couple in enzymes. There have been many structural studies of small molecules containing either the pyridinium ring found in NAD^+ or the dihydropyridine ring. In the case of the former, the pyridinium ring is almost invariably planar. In the case of NADH-type structures, there is more variability; some structures have a planar dihydropyridine ring, and some show some distortion.[16] Of most relevance to the current work are the structures reported[17] in 1988 by Benner and Dunitz. They determined solid-state structures of the *N*-propyl and *N*-methoxymethyl derivatives of NADH. In both of these structures, the dihydropyridine ring is essentially planar. This result is confusingly contradictory in light of the stereochemical demands of the reactions involving NADH since a planar ring offers no predisposition toward stereospecific hydride removal and suggests that the protein itself must stabilize any distortion of the NADH ring required to present the correct hydrogen atom to the substrate in the active enzyme.

To investigate the role of the internal hydrogen bond on hydride transfer from NADH to substrate and on the conformation of the nicotinamide ring, we performed electronic structure calculations, starting from the syn X-ray geometry with the hydrogen bond present, from which the structure was allowed to relax. Additionally, we performed calculations in which the nicotinamide ring was rotated into the anti conformation, where the hydrogen bond is absent. The differences between the syn and anti structures are striking. In the case of the syn conformation, both the MP2/6-31G(d,p) and B3LYP/6-31G(d,p) calculations reveal a nicotinamide ring which is still strongly puckered (Figure 2a) with the *pro-S* hydrogen atom in a pseudoaxial location. By contrast, for the anti conformation, both sets of calculations demonstrate that the nicotimamide ring has flattened substantially (Figure 2b). As calculations using only NADH with an internal hydrogen bond largely reproduce the observed distortion, it is clear that the presence of the internal hydrogen bond plays the principal role in forcing the NADH ring to adopt a puckered conformation.

(15) Guillot, B., Lecomte, C.; Cousson, A.; Scherf, C.; Jelsch, C. *Acta Crystallogr., Sect. D* **2001**, *57*, 981−989.

(16) A search of the CCDB reveals that there are 14 structures which are organic-only and possess *R* factors less than 10% which contain the dihydropyridine ring present in NADH. Of these 14 structures, seven exhibit a planar dihydropyridine ring (e.g., Cambridge Crystallographic Data Centre refcodes EXCMHP and GICHUV) and seven exhibit a boat conformation for the dihydropyridine ring (e.g., Cambridge Crystallographic Data Centre refcodes BECLUQ and WOCPUZ).

(17) Glasfield, A.; Zbinden, P.; Dobler, M.; Benner, S. A.; Dunitz, J. D. *J. Am. Chem. Soc.* **1988**, *110*, 5152−5157.

Scheme 1

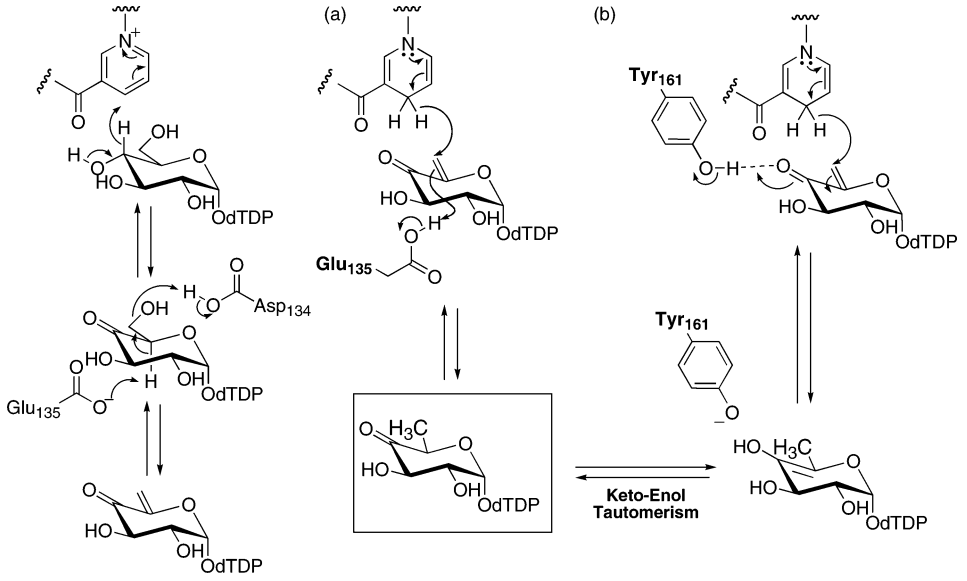

Previous work[17,18] has suggested that the syn nicotinamide conformation is a stronger reductant than the corresponding anti conformation, with the difference in reduction potential being driven by the degree of ring pucker and concomitant perturbation of the extended π system. In an attempt to quantify these differences between the syn and anti conformations, we calculated both the molecular electrostatic potential (ESP) for both conformations of NADH and at the degree of pucker observed in the X-ray structure. The results are summarized in Table 1. These calculations show that the area around the hydride that is transferred is significantly more negative (more nucleophilic) in the syn conformation (−8.2 kcal) compared to the anti conformation (+2.3 kcal). As the distortion increases toward that observed experimentally, the effect increases. While the absolute accuracy of these calculations cannot be relied upon, the trend is clear. The distortion appears to serve to significantly tune the redox potential of NADH, obviously desirable in an enzyme such as RmlB which has to oxidize a C−O bond and reduce a C═C double bond. Preliminary calculations suggest that the ring puckering may increase the reducing power of the NADH cofactor by around 25 mV. Although these results are preliminary, they suggest that the syn conformation of the NADH coupled with the stabilization of the ring pucker as described here provides a reductant which is tuned to the reaction.

Although our calculations using an internal hydrogen bond reproduce most of the distortion, the protein itself must have an effect, since the experimentally observed ring is slightly more distorted than the calculated one (Table 1). Examination (Figure 1c) of the X-ray structure of the RmlB active site reveals that the phenolic oxygen atom of Tyr161 is located directly above the nitrogen atom of the NADH dihydropyridine ring. In the first step of the reaction, Tyr161 becomes protonated. It therefore seemed possible that the tyrosine residue could hydrogen bond to the nitrogen atom of the NADH ring during hydride transfer to tune the redox potential of the coenzyme. To assess this possibility, we examined the effect on the electrostatic potential of the NADH ring when a phenol ring was placed within hydrogen-bonding distance of the NADH ring nitrogen atom. The addition of a hydrogen bond has little effect on the ESP around the transferred hydrogen atom (−8.9 kcal with vs −8.2 kcal without), and it is clearly less important than the internal hydrogen bond perturbing the redox potential. No other obvious interactions could be seen which might affect the ring structure.

Not only is hydride transferred in the final step, but a proton must also be added to the glucosene to give the product. In a concerted mechanism, hydride would be transferred to C6 and a proton to the carbanion at C5 (Scheme 1a). An alternative sequential mechanism proceeds through the conjugate addition of hydride to the terminus of the α,β-unsaturated system, forming an enolate (Scheme 1a). To distinguish these two possibilities, we undertook further calculations to elucidate which of these mechanisms, the single-step or a two-step mechanism, was most plausible using the model system shown in Scheme 2. We attempted to locate the transition structures for the synchronous addition of H^+ and H^- to the alkene (Scheme 2a) and the conjugate addition of hydride to the model α,β-unsaturated system (Scheme 2b). These calculations were performed at the MP2/6-31G(d,p) level of theory. These relatively high-level calculations do not locate a plausible transition structure for the synchronous transfer of hydride and proton (in the model the proton source is methanol). The sequential pathway (Scheme 2b) however, did offer a plausible transition structure (Figure 3a). Examination of the protein crystal structure shows that the enolate formed at O4 would be in close hydrogen-bonded contact with Tyr 161. Recalculating the model with a hydrogen bond to the forming enolate (Scheme 2c, Figure 3b) significantly lowers the activation barrier (by 6.2 kcal) of the process. This hydrogen bond to the enolate which forms after hydride transfer is thus very important to the mechanism. The pK_a of Tyr 161 in SDR enzymes is around 7,[19] and in the enzyme, we would expect a transfer of the phenolic proton from Tyr 161 to the enolate to give tyrosinate and the corresponding enol as the product. Whether the enol rearranges in the protein active site to give the keto sugar or

(18) Hajdu, J.; Sigman, D. S. *Biochemistry* **1977**, *16*, 2841−2846.

(19) Liu, Y.; Thoden, J. B.; Kim, J.; Berger, E.; Gulick, A. M.; Ruzicka, F. J.; Holden, H. M.; Frey, P. A. *Biochemistry* **1997**, *36*, 10675−10684.

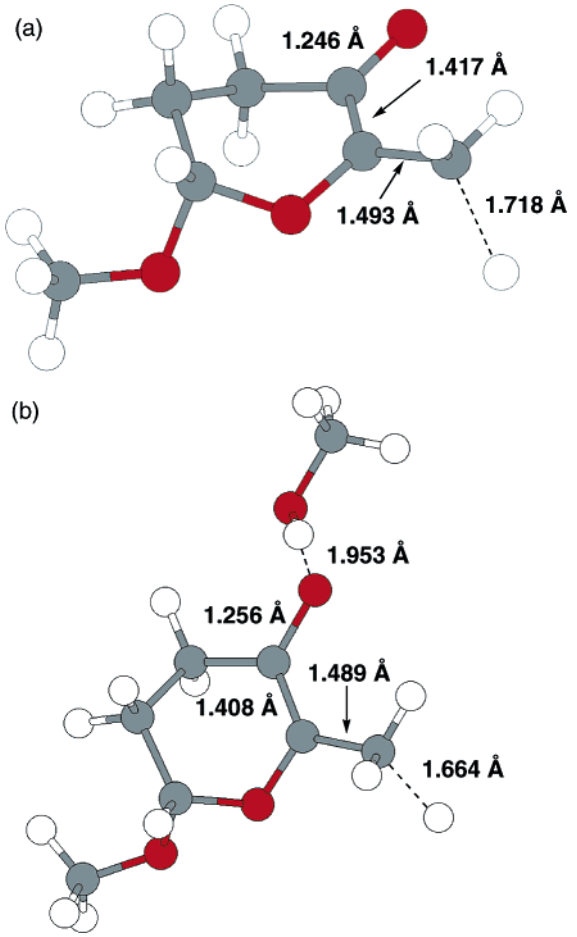

Figure 3. Structures of transition states calculated at the MP2/6-31G(d,p) level of theory for the model conjugate addition of hydride shown in Scheme 2. Carbon atoms are shown as gray spheres, oxygen as red, and hydrogen as white. In (b), methanol is included in the calculation as a model proton source. This transition state is lower in energy by 6.2 kcal compared to (a) with respect to the reagents.

Scheme 2

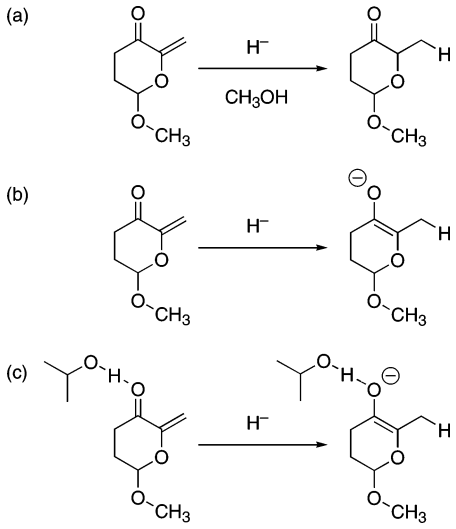

whether this occurs in solution after dissociation is not clear from our data.

Conclusions

This study is the first report of the direct observation of twisted boat conformation of NADH in an SDR enzyme. The degree of distortion is significantly greater than that seen in the LADH[7] structure where a hydroxide ion was found to control puckering. Calculations show that the dramatic puckering observed here results mainly from an internal hydrogen bond in NADH which is found in all *si* face structures of SDR enzymes to date. The hydrogen bond is not found in free NADH, and its occurrence is a result of the binding orientation of NADH in SDR enzymes. The effect of the puckering is to profoundly alter the nucleophilicity and redox potential of the hydride equivalent on the nicotinamide ring. This tuning of the redox behavior of the NADH is essential to the behavior of the enzymes which both abstract hydride and donate hydride, sometimes within the same reaction. Finally, the calculations establish the trajectory and sequence of proton and hydride transfer steps during the final reduction step of the RmlB enzyme.

Table 2. Data Collection and Refinement Statistics

	dTDP-xylose
wavelength (Å)	0.933
cell dimensions	
a (Å)	61.4
b (Å)	94.8
c (Å)	183.5
$\alpha = \beta = \gamma$ (deg)	90
resolution (Å)	34.7−1.5
space group	$P2_12_12_1$
no. of observations	2 567 266
no. of unique reflections	168 795
R_{merge}[a] (%)	11.6
overall completeness (%)	98.6
overall I/σ	4.3
I/σ highest-resolution shell	1.1
R_{factor}[b] (%)	17.0
R_{free}[c] (%)	19.9
root-mean-square deviation bonded distances (Å) (target value: 0.020)	0.019
rmsd angle bonded distances (Å) (target value: 0.020)	0.008
PDB accession code[d]	1OC2

[a] $R_{merge} = \sum_{hkl} \sum_i |I_i - \langle I \rangle| / \sum_{hkl} \sum_i \langle I \rangle$, where I_i is an intensity for the *i*th measurement of a reflection with indices *hkl* and $\langle I \rangle$ is the weighted mean of the reflection intensity. [b] $R_{free} = \sum_{hkl}||F_o(hkl)| - |F_c(hkl)|| / \sum_{hkl}|F_o(hkl)|$, where F_o and F_c are the observed and calculated structure factors, respectively. [c] R_{free} is the crystallographic R_{factor} calculated with 10% of the data that were excluded from the structure refinement. [d] Berman, H. M.; Battistuz, T.; Bhat, T. N.; Bluhm, W. F.; Bourne, P. E.; Burkhardt, K.; Feng, Z.; Gilliland G. L.; Iype, L.; Jain, S.; Fagan, P.; Marvin, J., Padilla, D.; Ravichandran, V.; Schneider, B.; Thanki, N.; Weissig, H.; Westbrook, J. D.; Zardecki, C.; *Acta Crystallogr., Sect. D* **2002**, *58*, 899−907.

Experimental Procedures

Sample Preparation, X-ray Data Collection. The cloning, overexpression, purification, and crystallization of *S. suis* serotype 2 RmlB have been described previously.[13] The dTDP-xylose complex data were collected at ESRF ID 14-2 using an ADSC Quantum 4 CCD detector. Data were processed with the program MOSFLM[20] and merged and scaled using the program SCALA from the CCP4 program suite.[21] Statistics are summarized in Table 1. Structure factors and atomic coordinates have been deposited with the RCSB (code 1OC2).

Spectrophotometric Analysis of the Crystals. Crystals containing dTDP-xylose and NADH were mounted in capillaries and examined using a single-crystal fiber-optic photodiode array microspectrophotometer with a xenon arc light source at room temperature. The spectra

(20) Leslie, A. G. W. *CCP4 and ESF-EACBM Newsletter on Protein Crystallography* **1992**, *26*.
(21) Collaborative Computational Project, Number 4. The CCP4 suite: Programs for protein crystallography. *Acta Crystallogr., Sect. D* **1994**, *50*, 760−763.

clearly demonstrate peaks at 280 and 340 nm, corresponding to the absorption maxima of the protein and NADH, thus confirming the presence of NADH in the protein crystals.

Refinement of the Complex. The RmlB from *S. suis* complexed with dTDP-xylose structure (PDB: 1KEP) and determined to a resolution of 1.8 Å was used as an initial model for refinement. Even at this resolution, the maps suggested the NADH was puckered; however, we felt there was insufficient data to model it this way, and the structure was refined using planar restraints on the nicotinimide ring. In the 1.5 Å refinement, the nicotinamide ring was initially set to have zero occupancy during refinement. The 1.5 Å model was refined with REFMAC 5[22] using isotropic and anisotropic thermal displacement parameters. The $F_o - F_c$ electron density maps show clearly that the density for the ring is not flat but distorted (Figure 1b). Refinement of an unrestrained nicotinamide ring leads to a puckered ring, but some of the bond distances within the ring are unrealistic. This is because the data are of insufficiently high resolution. Using chemical knowledge, we constructed a dictionary that restrained only the bond lengths and bond angles of the ring (Table 2). In effect, we allowed the ring to distort according to the X-ray data. Starting from a flat ring, refinement with this dictionary against the X-ray data results in a puckered ring that fits the electron density well. Geometry idealization (no X-ray) term results in a slightly puckered ring but with a different shape that does not fit the electron density. We regard this as unequivocal evidence that the experimental data are controlling the shape of the nicotinamide. The anisotropic motion of a C-4 atom perpendicular to the plane is quite pronounced, consistent with our view that the atom is flexible.

Ab Initio Electronic Structure Calculations. Molecular mechanics calculations and conformational searching were performed using the AMBER* or AMBER94 force fields and the GB/SA solvation model for water as implemented in Batchmin. Building and visualization were carried out using MacroModel.[23] Initially, low-energy conformations of NADH were generated using multiple Monte Carlo searches. Representative low-energy syn and anti structures were then used as starting points for the electronic structure calculations. Ab initio electronic structure calculations were performed at the MP2/6-31G-(d,p) level of theory using GAMESS[24] (the version dated September 6, 2001 (R2) was used in all calculations) or Jaguar[25] running on a variety of hardware platforms. Density functional theory calculations were performed at the B3LYP/6-31G(d,p) level of theory using Jaguar running on a variety of hardware platforms. Stationary points were characterized by appropriate thermodynamics calculations. Transition states located possessed one imaginary vibration corresponding to the reaction coordinate. Building, editing, and visualization were carried out using MOLDEN.[26]

Acknowledgment. The financial support of the Wellcome Trust (to J.H.N.) is gratefully acknowledged. J.H.N. is a BBSRC (U.K.) career development fellow. G.M. is a Wellcome Trust Fellow. We thank the reviewers for their constructive comments during the revision process.

Supporting Information Available: Calculated structures of syn and anti NADH and transition states (six PDB files). This material is available free of charge via the Internet at http://pubs.acs.org.

JA035796R

(22) Murshudov, G. N.; Vagin, A. A.; Dodson, E. J. *Acta Crystallogr., Sect. D* **1997**, *53*, 240−255.

(23) *MacroModel*, version 7.1, release 10; Schrödinger Inc.: Portland, OR, 2000.

(24) Schmidt, M. W.; Baldridge, K. K.; Boatz, J. A.; Elbert, S. T.; Gordon, M. S.; Jensen, J. H.; Koseki, S.; Matsunaga, N.; Nguyen, K. A.; Su, S. J.; Windus, T. L.; Dupuis, M.; Montgomery J. A. *J. Comput. Chem.* **1993**, *14*, 1347−1363

(25) *Jaguar*, version 4.1, release 53; Schrödinger Inc.: Portland, OR, 2000.

(26) Schaftenaar, G.; Noordik, J. H. *J. Comput.-Aided Mol. Des.* **2000**, *14*, 123−134.